In situ study of hydrogen silsesquioxane dissolution rate in salty and electrochemical developers

Running title: In situ study of hydrogen silsesquioxane development

Running Authors: Harry et al.

Katherine J. Harry[a), b), f)], Sebastian Strobel[a)], Joel K. W. Yang[a),c)], Huigao Duan[a),c)], Karl K. Berggren[a),d),e)]

[a)] Department of Electrical Engineering and Computer Science, Massachusetts Institute of Technology, Cambridge, Massachusetts 02139

[b)] Department of Chemical and Petroleum Engineering, The University of Kansas, Lawrence, Kansas 66044

[c)] Institute of Materials Research and Engineering, Agency for Science, Technology and Research, Singapore 117602

[d)] Kavli Institute of Nanoscience, Technical University of Delft, Delft, NL

[e)] American Vacuum Society member

[f)] Electronic mail: kharry@mit.edu

In order to better characterize the development of the electron-beam resist hydrogen silsesquioxane (HSQ), we used a quartz crystal microbalance (QCM) to study its rate of dissolution in situ. We determined the effect of both salt concentration and applied electric potential on the development rate of HSQ. The development rates were measured by spinning HSQ directly onto a quartz crystal resonator, and then developing in a QCM microfluidic module. In order to more directly observe the effect of electric potentials on HSQ development rate, a film of HSQ was partially cross-linked in an O_2 plasma asher then developed in the QCM flow module with a salt-free NaOH solution. As the partially cross-linked HSQ slowly developed, electric potentials were applied and removed from the

crystal allowing us to observe how the development rate increased upon the application of a positive electric potential. The increased development rate caused by both the addition of salt ions and a positive electric potential suggests that the rate may be limited by a build-up of negative charge on the HSQ.

I. INTRODUCTION

The fabrication of sub-10-nm-pitch structures using electron beam lithography with hydrogen silsesquioxane (HSQ) resist may be limited by the development of the resist material rather than exposure effects.[1] HSQ is a high-resolution resist material known for nm-length-scale line-edge roughness and improved etch-resistance relative to other electron-beam resists.[2, 3] Previous work demonstrated an increase in achievable resolution and developer contrast from the addition of salt into the developer solution.[4] Moreover, salt was shown to reduce the self-limiting nature of the HSQ development process.[5, 6] Additional research has shown improvements in achievable resolution using hot development,[7] a two-step method involving an HF dip,[8] and alternate developer chemistries.[9]

It was hypothesized that the enhancement associated with adding salt to developer could be due to an increase in development rate caused by surface charge screening.[1] Furthermore, there was no explanation for why patterning below 9-nm pitch was not possible in these experiments. It is possible that charge screening, especially in high-aspect-ratio nm-length-scale trenches, inhibits dissolution to the point of stopping. An electrostatic surface charge effect has been reported for photoresist development processes.[10] Additionally, electric fields have been used to decrease line-edge roughness for structures patterned in photoresist.[11] However, the effect of surface charge on

development rate and developer contrast in this HSQ resist system has not yet been studied even on a macroscopic scale.

During development, the alkaline developer solution reacts with HSQ to form negatively charged HSQ ions that are soluble in the aqueous solution. This process may result in a build-up of negative charge on the surface of the HSQ features. This negative charge will repel the hydroxyl anions, reducing their concentration within a distance on the order of the Debye length (~ 1 nm) of the HSQ surface. This reduced concentration, in turn, may result in a decreased development rate, particularly in nm-length-scale trenches. When salt is added to the developer solution, the additional Na^+ ions might screen this negative surface charge allowing the alkaline developer ions to approach the surface resulting in an increased development rate. [12]

This paper isolates the surface charge effect by applying a positive electric potential directly to the substrate during development. A quartz crystal microbalance (QCM) serves as an effective tool to compare the effect on the development rate of HSQ of surface charge biasing due to an applied electric potential against the charge screening caused by salt. Additionally, surface profilometry and conventional imaging techniques were used to support the QCM results. The QCM was used to study the development rate of HSQ in salty developer solution (0 – 20% NaCl in 1% NaOH) and using electrochemical development techniques (0 – 2.5 V in 1% NaOH). We found that the development rate of HSQ increased upon the application of a positive electric potential and with the addition of salt. However, the increased development rate does not result in increased developer contrast.

The quartz crystal microbalance measures the resonance frequency of a quartz crystal in real time. It has been used to study the dissolution of molecular resist for EUV lithography,[13] the swelling of photoresist[14] and polymer nanocomposites,[15] and the development of fluoropolymer-based resist solutions.[16] A correlation exists between the change in the frequency and the mass of the resonator, allowing for in situ monitoring of the mass. The Voight model permits analysis of the change of mass in the presence of viscoelastic drag, and was used to analyze the results presented here. [17]

II. EXPERIMENTAL

Three distinct methods were used to study the development rate of HSQ:

1. a QCM to monitor dissolution rates in real-time;
2. cross-section scanning-electron micrographs (SEMs) of line features on silicon to observe differences in development rates around nanostructures; and
3. dose matrices exposed into HSQ on silicon to measure developer contrast.

For the first method, gold-plated quartz crystal resonators were purchased from the QCM manufacturer, Q-sense. The crystals were cleaned by rinsing in acetone, methanol and isopropanol followed by 5 min in a UV-ozone generator. Once clean, approximately 100 nm of HSQ was spun onto the crystals using Dow-Corning 6% HSQ in MIBK at 5 krpm for 60 s. In order to slow down the development rate enough to observe variation of in-situ development rates, prior to development, the HSQ was partially cross-linked by placing the crystals in an O_2 plasma asher for 30 s at 150 W.

Silicon samples were prepared for line exposures by spinning approximately 175 nm of Dow Corning 6% HSQ onto a highly p-doped silicon wafer. A pattern of 500-µm-long lines at linear dose densities ranging from 1.4 to 4.5 nC/cm was exposed onto the samples

using the Raith 150 electron beam lithography tool at the SEBL facilities at MIT. The exposure energy was 10 keV with an aperture diameter of 30 µm.

Samples were prepared for dose matrix measurements by spinning 170 nm of HSQ onto a highly p-doped silicon wafer. A dose matrix made up of forty, 10 µm × 40 µm features was exposed with an aerial dose density ranging from 100 – 2050 $\mu C/cm^2$ using the Raith 150 electron beam lithography tool at an energy of 30 keV.

The silicon samples were placed in a custom acrylic sample holder designed to control the sample area exposed to solution during development. The sample was sandwiched between two acrylic slides with a ¼”-diameter hole exposed to solution as shown in Fig. 1a. It was then developed using the setup illustrated in Fig. 1b. The electric potential was applied to the substrate in reference to a Ag/AgCl electrode. The current between the counter electrode and the sample was measured using a 4 point measurement technique. After development, the samples exposed with the line pattern were cleaved and mounted on a tilting stage for cross-section imaging. The Raith 150 electron beam lithography tool was used to image the structures at 10 keV with a 9 mm working distance. A surface profilometer was used to measure the heights of the features in the dose matrix for developer contrast observations.

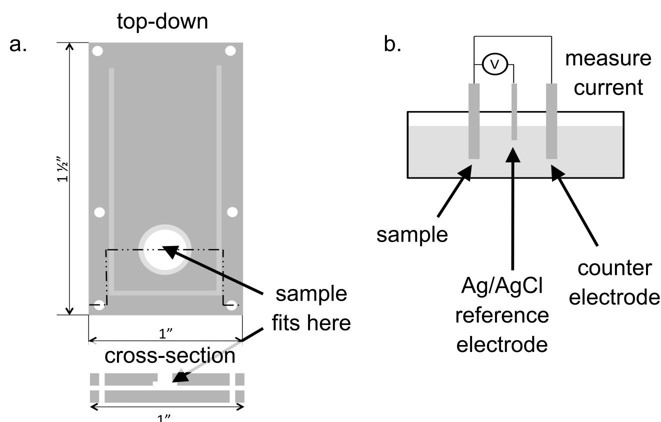

Figure 1. (a) Schematic diagram of sample holder. This holder limited the area of the silicon wafer that was exposed to solution during electrochemical development. The wafer was sandwiched between two acrylic slides using fluorosilicone O-rings to prevent developer solution from contacting the slide on any place other than the ¼" diameter central hole. (b) Schematic of experimental setup for immersion development of sample with a reference and counter electrode.

The quartz crystals were developed in a microfluidic module designed to flow solution over the crystal while measuring the resonance frequency of the crystal. A different, electrochemical microfluidic module was used to develop the samples with an applied electric potential. The QCM development setup is illustrated in Figure 2.

A control experiment was completed to compare the development rate of HSQ measured using the basic flow module to the electrochemistry flow module under the same development conditions with no applied potential. Despite geometric differences in the flow chambers, the rates were within 0.5 nm/s of each other relative to an overall development rate on the order of 6 nm/s.

Typically, QCM can only be used to measure changes in mass over long time intervals due to the slow flow rate (150 μL/min) and thus long mixing time upon fluid change (~ 1 min). Thus, there was concern about using the method to study such a rapid

process as HSQ development. Nonetheless, the method proved a useful tool to compare development rates but was not ideal for giving absolute development rate values.

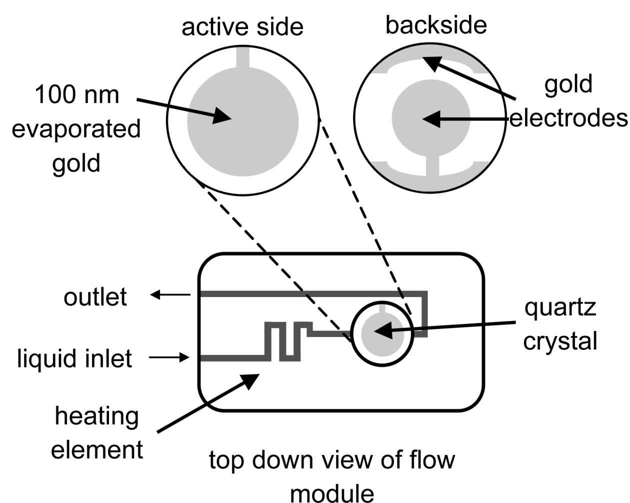

Figure 2. Schematic of QCM apparatus. To make in situ development rate measurements, a thin layer of HSQ was spun directly onto the active side of the quartz crystal resonator. An oscillating electric field at the resonance frequency was applied to the gold electrodes. Its resonance frequency increased as mass was removed from the crystal.[18] For electrochemical studies, a controlled electric potential was applied to the evaporated gold layer beneath the HSQ on the active side. A peristaltic pump was used to control the flow rate of developer solution into the QCM microfluidic module. The solution passed over a temperature sensor and controller before contacting the active side of the crystal. O-rings prevented the solution from contacting the backside of the crystal. In the electrochemistry module, a platinum counter electrode and Ag/AgCl reference electrode were used with a potentiostat to control the applied electric potential.

Before starting each run, the initial resonance frequency of the crystal was determined by "pinging" the crystal with a range of frequencies and measuring its amplitude response. Six overtones were found in addition to the base resonance frequency. Monitoring these overtones improves the reliability of the data relative to simply

monitoring the central resonance frequency, and is essential to the analytic models. Deionized (DI) water was pumped into the microfluidic chamber using a peristaltic pump, and the temperature of the solution was controlled with a heating element inside the microfluidic chamber. After starting the run, the change in the resonance frequency and the dissipation was measured at each of the overtones at a rate of ~200 data points per second.

For the measurements with salty developer but without additional potential, 1% NaOH aqueous developer solution with a salt concentration ranging from 1 – 20% NaCl replaced the DI water in the flow module. After the development was finished, the solution was switched back to DI water. For the electric potential development measurements, a voltage ranging from 0 – 2.5 V was applied to the substrate relative to a Ag/AgCl reference electrode while running DI water over the sample. With the voltage still applied, the DI water was then replaced by salt-free 1% NaOH developer solution. After development, the solution was switched back to DI water and the electric potential was turned off. For the final set of measurements, 1% NaOH was pumped over the sample. An electric potential of +2.5 V was applied to the sample for 30 s then turned off. After 95 s of normal development, a second electric potential of +4 V was applied to the sample. This experiment permitted direct comparison of development rate with and without an electric potential within a single development run.

III. RESULTS AND DISCUSSION

Figure 3 shows a top-down SEM of 11-nm-pitch nested-L structures fabricated according to a standard process.[4] Although our ultimate goal was to improve on this result, metrology at this length scale is challenging, and thus the process was optimized at a

longer length scale in the hopes that future work could take advantage of the optimized process.

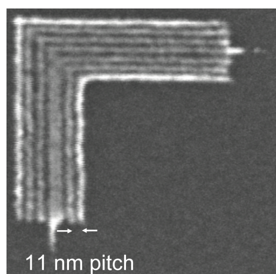

Figure 3. Top-down scanning electron micrograph of 11-nm pitch nested-L structures in HSQ resist fabricated using electron beam lithography and a standard salty developer process (1% NaOH and 4% NaCl).

The cross-section images in Fig. 4 of a line pattern exposed in HSQ on silicon show deeper trenches when developed with a +5 V applied potential than with no potential. The two samples were both developed for 45 s in a salt-free 1% NaOH solution. Deeper trenches, indicating a faster development rate, were observed under the application of an electric potential.

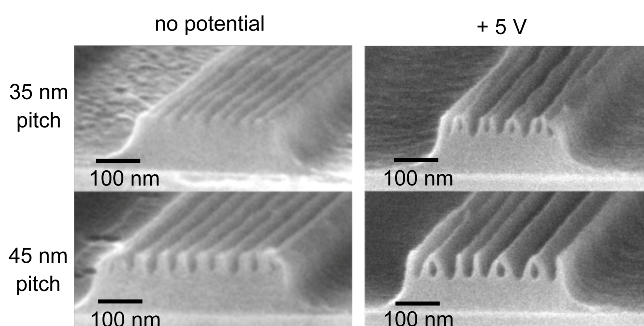

Figure 4. Scanning electron micrographs comparing developed resist cross sections with and without a potential applied during development. A Raith 150 electron beam lithography tool was used to expose a line pattern into HSQ on highly p-doped silicon. An increase in resist removed between the features was evident when a positive 5 V potential was applied to the substrate surface during development in 1% NaOH solution.

The quartz crystal microbalance data support these results by showing that the development rate nearly doubled when a +2.5 V electric potential was applied to the substrate during development. Figure 5 shows that when a positive electric potential was applied to the crystal during development, the development rate increased from 5.5 nm/s at 0 V to 9 nm/s at 2.5 V. Similarly, when NaCl was added to 1% NaOH developer solution, the development rate increased from 6 nm/s with 0% NaCl to 9 nm/s with 20% NaCl. Furthermore, Fig. 6 illustrates the effect of the applied potential on the development rate as it was monitored in real-time. Again, the rate nearly doubled upon the application of +2.5 V.

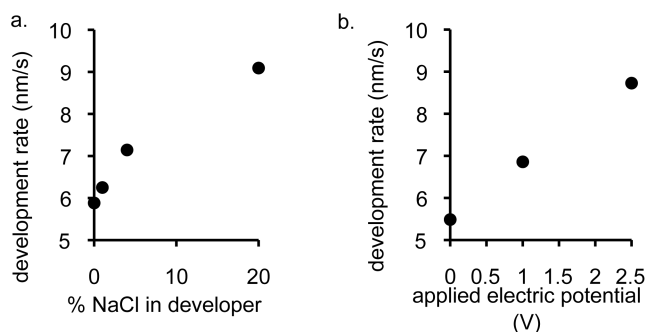

Figure 5. Comparison of the dependence of development rate on salt concentration and applied potential. The development rate of HSQ in salty developer and electrochemically-enhanced developer was determined with a QCM. (a) 96 nm of HSQ resist was spun onto a gold-plated quartz crystal. The crystal was mounted in a QCM flow module and developed with 1% NaOH mixed with varying concentrations of NaCl with no applied electric potential. The development rate increased as the concentration of NaCl increased. (b) Similarly, the development rate increased with the strength of the applied positive electric potential in 1% NaOH solution with no NaCl.

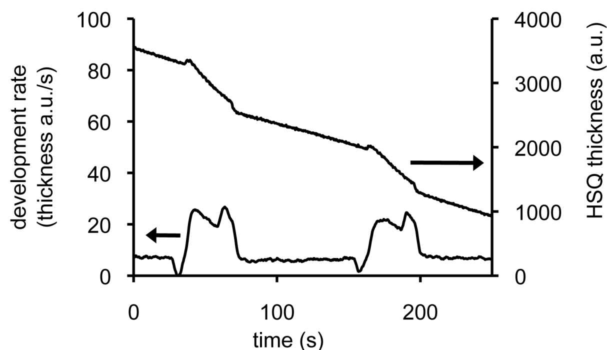

Figure 6. In-situ observation of dependence of development rate on applied voltage. A quartz crystal was coated with 96 nm of HSQ then placed in an O_2 plasma asher for 30 s at 150 W in order to partially crosslink the HSQ film. 1% NaOH developer solution was passed over the HSQ in a microfluidic module. A positive electric potential of 2.5 V was applied to a gold electrode beneath the HSQ from 35 s to 65 s causing a sharp increase in the development rate. From 160 s to 190 s, 4 V was applied to the crystal.

Previous researchers have suggested that a negative surface charge builds up on HSQ features during development.[1] The development may proceed by the following reaction between the HSQ and the hydroxyl ions in the developer: [4]

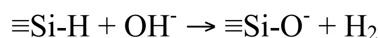

$$\equiv Si\text{-}H + OH^- \rightarrow \equiv Si\text{-}O^- + H_2$$

When salt is added to the developer solution, the additional charge carriers screen the negative charge, reducing the Debye length and allowing NaOH developer molecules to approach the HSQ features, effectively increasing the developer concentration at the HSQ surface. Likewise, when a positive electric potential is applied to the substrate during development as shown in Fig 4, 5b, and 6, the charge may thin the electrical double layer at the HSQ–developer interface, yielding a similar rate-enhancement effect as is observed when salt is added to the developer. In this case, the development rate increases because

the concentration of NaOH anions at the HSQ surface increases as the repulsive surface charge is reduced.

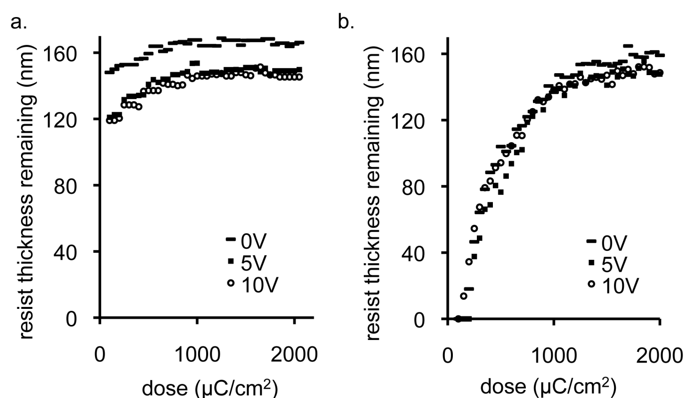

Figure 7. Resist thickness remaining vs. dose. A dose matrix was exposed into a 170 nm thick layer of HSQ on highly p-doped silicon. (a) samples were developed for 15 s in 0.3% NaOH 1.3% NaCl salty developer solution, then the resist thickness remaining was measured using a surface profilometer. (b) the samples were developed for an additional 60 s (totaling 75 s) then measured. When an electric potential was applied to the sample, more resist was removed in the first 15 s than was removed with conventional development, indicating an increased development rate. However, after full development, no increase in contrast was observed. Similar results to (b) were observed in 1% NaOH solution without NaCl, but are not shown, the scenario described in (a) was not tested without NaCl.

However, Fig. 7 shows that the increase in development rate caused by the applied electric potential does not translate to an increase in developer contrast. By applying an electric potential instead of adding salt, we were able to study the effect of charge on HSQ development in isolation from the ionic molecular interactions. We found that in this case, the potential increased the reaction rate, but the contrast remained the same. As we will

now discuss, this result suggests that the achievable contrast is controlled by the reaction equilibrium instead of its kinetics.

When electrolytes are added to a solution, they tend to alter the relative solubility of the solution components.[19] In the case of HSQ development, adding NaCl may increase the developer contrast by reducing the amount of partially cross-linked HSQ dissolved in solution.[4] This contrast enhancement may be the result of the salt decreasing the solubility of the partially cross-linked HSQ that was exposed above the threshold dose of the process. In biological sciences this "salting out" technique is often used to decrease the solubility of proteins in water.[20] This process parallels the HSQ development process, where the salt reduces the amount of partially cross-linked HSQ in solution. Thus, adding salt to the solution potentially results in two main effects on the development system. First, it increases the development rate through charge screening. Secondly, it increases the developer contrast through altering the solid-liquid chemical equilibrium (salting out).

This interpretation of our results thus confirms the notion that surface charge affects the development rate, as was suspected from the salty development work. However, it also implies that surface charge does not play a major role in the macroscopic (micrometer-length-scale) resist contrast. Of course, it is still possible that resist-development contrast at the nm length scale could be impacted by surface charge effects.

IV. SUMMARY AND CONCLUSIONS

In order to increase the achievable resolution of features patterned using an electron beam lithography tool, it is important to understand the electrical and chemical effects that govern the development process. From this work, we understand that adding positive charge to the system through either ions or an electric potential will increase the reaction

rate. Furthermore, we understand that the contrast enhancement yielded by the salt is not simply an effect of the charge screening but could instead be the result of molecular interactions between the salt and reacting species.

ACKNOWLEDGMENTS

The authors would like to thank Jim Daley and Mark Mondol for making this work possible by sharing their fabrication expertise, and Dr. Michael Rooks, for helpful conversations. The Scanning Electron Beam Lithography facility at the Research Laboratory of Electronics at MIT (SEBL at RLE) was used for sample exposures and imaging and the Nanostructures Laboratory (NSL) at MIT was used for sample processing. Financial support was provided by the National Science Foundation, the Center for Materials Science and Engineering, the Materials Processing Center at MIT, and the King Abdulaziz Center of Science and Technology.

[1] J. K. W. Yang, B. Cord, H. Duan, D. C. Joy, J. Klingfus, K. K. Berggren, J. Vac. Sci. Technol. B **27**, 2616 (2009).

[2] H. Namatsu, Y. Takahashi, K. Yamazaki, T. Yamaguchi, M. Nagase, K. Kurihara, J. of Vac. Sci. Technol. B **16**, 69 (1998).

[3] L. O'Faolain, M. V. Kotlyar, N. Tripathi, R. Wilson, T. F. Krauss, J. of Vac. Sci. Technol. B **24**, 336 (2006).

[4] J. K. W. Yang, K. K. Berggren, J. of Vac. Sci. Technol. B **25**, 2025 (2007).

[5] S. W. Nam, M. J. Rooks, J. K. W. Yang, K. K. Berggren, H. M. Kim, M. H. Lee, K. B. Kim, J. H. Sim, D. Y. Yoon, J. of Vac. Sci. Technol. B **27**, 2635 (2009).

[6] J. Kim, W. L. Chao, B. Griedel, X. G. Liang, M. Lewis, D. Hilken, D. Olynick, J. of Vac. Sci. Technol. B **27**, 2628 (2009).

[7] M. Haffner, A. Haug, A. Heeren, M. Fleischer, H. Peisert, T. Chasse, D.P. Kern, J. of Vac. Sci. Technol. B **25**, 2045 (2007).

[8] H.-S. Lee, J.-S. Wi, S.-W. Nam, H.-M. Kim, and K.-B. Kim, J. Va. Sci. Technol. B **27**, 188 (2008).

[9] G. M. Schmid, L. E. Carpenter, J. A. Liddle, J. of Vac. Sci. Technol. B **22**, 3497 (2004).

[10] G. M. Schmid, S. D. Burns, P. C. Tsiartas, C. G. Willson, J. of Vac. Sci. Technol. B **20**, 2913 (2002).

[11] R. Bristol, H. Cao, M. Chandhok, R. Measgly, V. Ramachandrarao, U.S. Patent No. 7,374,867 (May 20, 2008).

[12] J. K. W. Yang, B. Cord, H. Duan, K. K. Berggren, J. Vac. Sci. Technol. B **27**, 2622 (2009).

[13] M. Toriumi, J. Santillan, T. Itani, T. Kozawa, S. Tagawa, J. Vac. Sci. Technol. B **25**, 2486 (2007).

[14] H. V. Tran, E. Hendrickx, F. Van Roey, G. Vandenberghe, R. H. French, J. Micro/Nanolith. MEMS MOEMS **8**, 033006 (2009).

[15] D. J. Schmidt, F. C. Cebeci, Z. I. Kalcioglu, S. G. Wyman, C. Ortiz, K. J. Van Vliet, P. T. Hammond, ACS Nano **3**, 2207 (2009).

[16] M. Toriumi, T. Yamazaki, T. Furukawa, S. Irie, S. Ishikawa, T. Itani, J. Vac. Sci. Technol. B **20**, 2909 (2002).

[17] M.V. Voinova, M. Rodahl, M. Jonson, B. Kaserno, Physica Scripta **59**, 391 (1999).

[18] G. Wang, M. Rodahl, M. Edvardsson, S. Svedhem, G. Ohlsson, F. Hook, B. Kasemo, Review of Scientific Instruments **79**, 075107 (2008).

[19] E. W. Washburn, *An introduction to the principles of physical chemistry*, (McGraw-Hill, New York, 1921). Vol. 2.

[20] R. Chang, *Physical chemistry for the biosciences*, edited by J. Murdzek (University Science Books, 2005), pp. 170.